

Controlled preparation and electron emission properties of three-dimensional micropatterned aligned carbon nanotubes

Ajeeta Patil, Toshiyuki Ohashi, Alper Buldum, and Liming Dai

Citation: *Appl. Phys. Lett.* **89**, 103103 (2006); doi: 10.1063/1.2345253

View online: <http://dx.doi.org/10.1063/1.2345253>

View Table of Contents: <http://apl.aip.org/resource/1/APPLAB/v89/i10>

Published by the [American Institute of Physics](#).

Additional information on *Appl. Phys. Lett.*

Journal Homepage: <http://apl.aip.org/>

Journal Information: http://apl.aip.org/about/about_the_journal

Top downloads: http://apl.aip.org/features/most_downloaded

Information for Authors: <http://apl.aip.org/authors>

ADVERTISEMENT

**AIP**Advances

Submit Now

**Explore AIP's new
open-access journal**

- **Article-level metrics
now available**
- **Join the conversation!
Rate & comment on articles**

Controlled preparation and electron emission properties of three-dimensional micropatterned aligned carbon nanotubes

Ajeeta Patil

Department of Polymer Engineering, College of Polymer Science and Polymer Engineering, University of Akron, Akron, Ohio 44325

Toshiyuki Ohashi

Honda Research Institute USA, Inc., 1381 Kinnear Rd., Suite 116, Columbus, Ohio 43212

Alper Buldum

Department of Physics, College of Arts and Sciences, University of Akron, Akron, Ohio 44325

Liming Dai^{a)}

Department of Chemical and Materials Engineering, School of Engineering, University of Dayton, 300 College Park, Dayton, Ohio 45469-0240 and UDRI, University of Dayton, 300 College Park, Dayton, Ohio 45469-0240

(Received 6 May 2006; accepted 24 July 2006; published online 5 September 2006)

The authors have developed a simple, but very effective and versatile, dry contact transfer technique for controlled preparation of three-dimensional (3D) perpendicularly aligned carbon nanotube micropatterns with region-specific tube lengths. The 3D micropatterned aligned carbon nanotubes were demonstrated to show a stepwise electron emission behavior, providing an effective means for developing multifunctional electron emitters with tailor-made field emission characteristics. © 2006 American Institute of Physics. [DOI: 10.1063/1.2345253]

Soon after the discovery of carbon nanotubes by Iijima in 1991,¹ de Heer *et al.*,² Rinzler *et al.*,² and Saito *et al.*² reported the field emission from carbon nanotubes. Since then, electron emission properties of various carbon nanotubes, either in a patterned or nonpatterned form, have been studied extensively.³ Of particular interest, electron emissions from vertically aligned carbon nanotubes (ACNTs) with a homogenous tube length, either in a two-dimensionally (2D) micropatterned or nonpatterned form, were reported,^{4–10} along with some peculiar emission features (e.g., the edge effect for patterned carbon nanotube arrays).¹⁰ As a result, carbon nanotubes have been exploited as field emitting materials for display applications.^{11–16} As far as we are aware, however, the electron emission from three-dimensional (3D) ACNT micropatterns has not been discussed in the literature largely because of the lack of an effective method for preparing 3D ACNT micropatterns with a region-specifically controllable tube length.^{17–19}

On the other hand, we, along with others, have devised various micropatterning methods, including photolithography,^{20–22} soft lithography,^{23,24} and contact transfer,^{25,26} for producing 2D ACNT micropatterns. On our further study in patterning of ACNTs by the dry contact transfer method,²⁶ we found that 3D ACNT micropatterns with a region-specifically controllable tube length can be prepared through the dry contact transfer with slight modification. Here, we report the detailed procedures for the formation of 3D ACNT micropatterns by the modified dry contact transfer method, along with electron emission characteristics of the 3D ACNT micropatterns thus produced.

To demonstrate the 3D ACNT micropatterning, we first synthesized nonpatterned ACNT array with a homogenous tube length on a quartz glass plate by pyrolysis of FePc in

Ar/H₂ atmosphere at 1100 °C according to our published procedure.^{25,27} As shown in Fig. 1, the as-synthesized ACNT array was then coated with a micropatterned metal (e.g., Al, Ag, and Au) layer by patterned sputter coating (or thermal evaporation) through a physical mask [e.g., a transmission electron microscopy (TEM) grid, *top left* of Fig. 1]. The thickness of the metal coating was controlled by changing the coating conditions (e.g., deposition time). After a desirable coating thickness was obtained, an adhesive film (e.g., a 3M Scotch tape) was pressed onto the ACNT array prepatterned with the metal layer (*top right* of Fig. 1), followed by peeling off the Scotch tape with the ACNT film from the quartz substrate in a dry state and turning over the Scotch-supported ACNT film upside down. Finally, 3D ACNT micropatterns with a region-specific tube length were produced by simply pushing up the Scotch tape underneath the metal-patterned area against the rest part of the ACNT film (*bottom right* of Fig. 1).

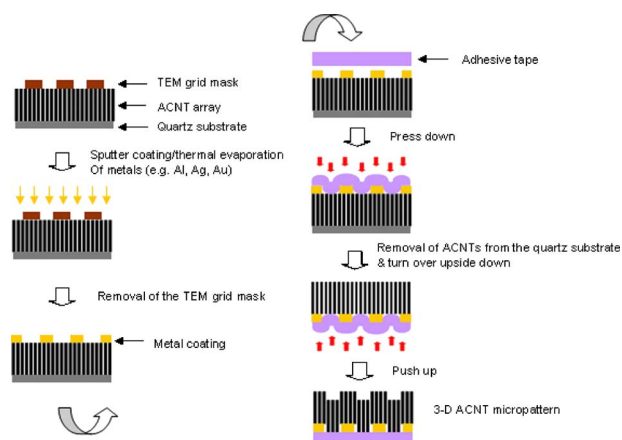


FIG. 1. (Color online) Procedures for the fabrication of 3D ACNT micropatterns.

^{a)}Electronic mail: ldai@udayton.edu

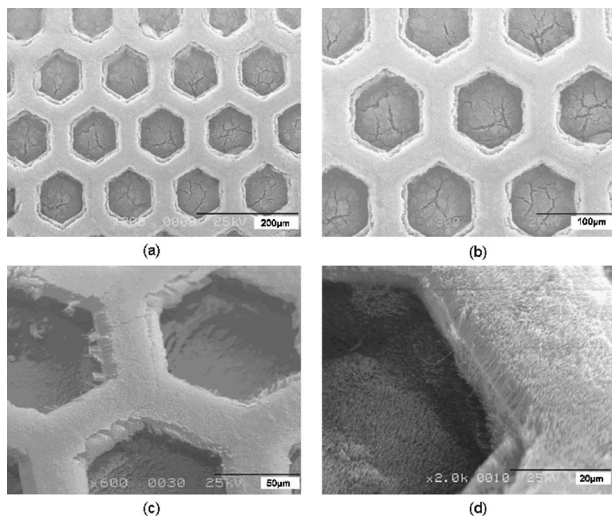


FIG. 2. [(a) and (b)] SEM micrographs of the 3D ACNT micropattern prepared by the modified dry contact transfer technique and [(c) and (d)] the same as for (a) and (b), but under higher magnifications. Scale bars: (a) 200 μm , (b) 100 μm , (c) 50 μm , and (d) 20 μm .

3D ACNT micropatterns thus prepared were characterized by scanning electron microscopy (SEM). Figures 2(a) and 2(b) reproduce a typical 3D ACNT micropattern prepared by the dry contact transfer using a TEM grid mask with hexagonal windows of a 100 μm width and a 50 μm wide grid bar, which shows layered hexagonal micropatterns. The 3D micropatterned ACNTs are clearly evident by inspection of Figs. 2(a) and 2(b) under higher magnifications [Figs. 2(c) and 2(d)]. Figures 2(c) and 2(d) also show that the tube height difference in the 3D micropatterned ACNTs is ca. 10 μm , in consistent with the thickness of the micropatterned metal layer. The alignment of the transferred carbon nanotubes is largely retained in both of the layered structures.

The interesting electron emitting properties reported for both nonpatterned and 2D micropatterned ACNT arrays^{4–10} prompted us to measure electron emissions from these 3D micropatterned ACNT arrays. To construct the 3D micropatterned ACNTs for electron emission measurements, we prepared a conducting electrode by depositing a thin layer of Au homogeneously over the whole nanotube array either before or after the metal patterning (cf. Fig. 1). Electron emitting characteristics of the 3D ACNT micropatterns were then measured using customer-made setup according to the published procedure,^{28,29} using a spacer with a relatively small window size of about $2 \times 2 \text{ mm}^2$ to cover the micropatterned emitting area. The electron emitting property of the as-synthesized (nonpatterned) ACNT array was also measured as reference. The obtained I - E plots for the as-synthesized and 3D micropatterned ACNTs are given in Fig. 3. As can be seen in Fig. 3, the emission behavior of the 3D micropatterned ACNTs [Fig. 3(b)] shows a deviation from its nonpatterned counterpart [Fig. 3(a)].

The silent feature to note is that the I - E curve for the 3D micropatterned ACNTs shows a stepwise emission with two possible turn-on voltages. The second turn-on voltage coincides with that observed in the case of nonpatterned ACNT (i.e., 1.6 $\text{V}/\mu\text{m}$). The lower turn-on voltage observed in Fig. 3(b) is, most probably, resulted from the elevated ACNT emitters in the 3D architecture because the distance between the two electrodes was determined from the surface of the

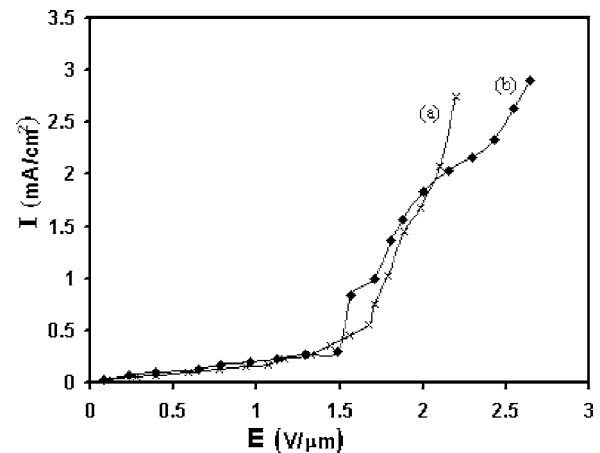


FIG. 3. I - E curves for electron emissions from the (a) nonpatterned ACNT array (\times) and (b) 3D micropatterned ACNT array (\blacklozenge).

bottom electrode to the opposite electrode. Because the elevated ACNTs are more close to the opposite electrode, they started emitting electrons at a lower overall voltage than those emitted from the base ACNTs, and hence an early increase in the current density. Above the second turn-on voltage, the emission behavior becomes similar with that of the nonpatterned ACNTs. The decay in emission seen in Fig. 3(b) at voltages above ca. 2.1 $\text{V}/\mu\text{m}$ is probably due to possible field-induced damage of some elevated ACNTs, which reduced the total number of effective nanotube emitters and hence the weaker emission current with respect to Fig. 3(a).

In view of the above peculiar emission behavior of the 3D micropatterned ACNTs and our earlier results of a field-enhanced emission current and reduced turn-on voltage for electron emitters based on nonpatterned plasma-polymer-coated ACNT arrays,^{28,29} we moved one step further in this study to test if the stepwise emission seen above could also be introduced by patterned plasma modification of the ACNT emitters while retaining their uniform height. The plasma patterned ACNT array was performed on an as-synthesized FePc-generated ACNT array by plasma polymerization of hexane with the monomer pressure of 0.25 Torr at 250 kHz and 30 W for 90 s through the hexagonal TEM grid.³⁰ For comparison, an ACNT array was also treated by hexane-plasma polymerization under the same condition, but without using the TEM grid for patterning.

Figures 4(a) and 4(c) show changes in the I - E curves for the nonpatterned ACNT array upon plasma polymerization of hexane. In consistent with our previous results,^{28,29} the hexane-plasma coating reduced the turn-on electric field from ca. 1.6 to ca. 1.0 $\text{V}/\mu\text{m}$, coupled with a concomitant increase in the emission current at a constant E due to an enhanced field at the nanotube tips while insulating their wall with the nonconducting plasma polymer coating. Like the 3D micropatterned ACNTs, the I - E curve for the plasma-patterned ACNT array in Fig. 4(b) shows a stepwise emission with two possible turn-on voltages. This behavior can be attributed to sequential electron emissions from the plasma-polymer-coated ACNTs and pure ACNTs within the same plasma-patterned ACNT array. In this particular case, the plasma-coated ACNTs started emitting electrons at the first turn-on voltage of ca. 1.4 $\text{V}/\mu\text{m}$, followed by the field emission from the pure ACNTs turned on at ca. 1.7 $\text{V}/\mu\text{m}$, leading to a stepwise jump in the I - E curve [Fig. 4(b), cf. Fig.

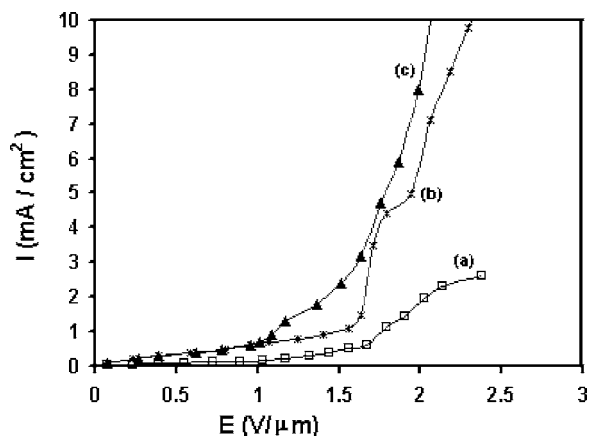


FIG. 4. I - E curves for a (a) pure ACNT array (\square)—note that a different ACNT array from that of Fig. 3(a) was used, (b) plasma-patterned ACNT array (\times), and (c) nonpatterned plasma treated ACNT array (\blacktriangle).

3(b)]. Therefore, the above observed stepwise emissions are rather general for multicomponent electron emitters.

In summary, we have developed a simple, but very effective and versatile, dry transfer technique for controlled preparation of 3D perpendicularly aligned carbon nanotube micropatterns with region-specific tube lengths. We have further used the 3D micropatterned aligned carbon nanotubes as electron emitters. We found a stepwise electron emission behavior for the 3D micropatterned aligned carbon nanotubes and their 2D counterparts prepared by plasma patterning. The observed stepwise electron emission was demonstrated to be rather versatile for multicomponent emitters, providing an effective means for developing multifunctional electron emitters with tailor-made field emission behaviors. With the recent rapid development in nanoscience and nanotechnology, these 3D micropatterned and plasma-patterned aligned carbon nanotube electron emitters reported in this study could be very useful in many multidimensional and multifunctional systems, including patterned electron emitting displays, multianalyte sensors, multichannel microreactors, and microfluidic devices.

The authors thank Honda R&D, Co., Ltd. and AFOSR (FA9550-06-1-0384) for financial support.

¹S. Iijima, *Nature (London)* **354**, 56 (1991).

²W. A. de Heer, A. Chatelain, and D. Ugarte, *Science* **270**, 1179 (1995); A. G. Rinzler, J. H. Hafner, P. Nikolaev, L. Lou, S. G. Kim, D. Tomanek, P.

Nordlander, D. T. Colbert, and R. E. Smalley, *ibid.* **269**, 1550 (1995); Y. Saito, K. Hamaguchi, K. Hata, K. Uchida, Y. Tasaka, F. Ikazaki, M. Yumura, A. Kasuya, and Y. Nishina, *Nature (London)* **389**, 554 (1997).

³K. Kajiwara and Y. Saito, in *Carbon Nanotechnology: Recent Developments in Chemistry, Physics, Materials Science and Device Applications*, edited by L. Dai (Elsevier, Amsterdam, 2006), pp. 577–609

⁴T. Ikuno, S. Honda, H. Furuta, K. Aoki, T. Hirao, K. Oura, and M. Katayama, *Jpn. J. Appl. Phys., Part 1* **44**, 1655 (2005).

⁵G. Takeda, L. Pan, S. Akita, and Y. Nakayama, *Jpn. J. Appl. Phys., Part 1* **44**, 5642 (2005).

⁶J. T. Li, W. Lei, X. B. Zhang, B. P. Wang, and L. Ba, *Solid-State Electron.* **48**, 2147 (2004).

⁷W. J. Yu, Y. S. Cho, G. S. Choi, and D. Kim, *Nanotechnology* **16**, S291 (2005).

⁸Y. Huh, J. Y. Lee, and C. J. Lee, *Thin Solid Films* **475**, 267 (2005).

⁹C. C. Chuang, J. H. Huang, C. C. Lee, and Y. Y. Chang, *J. Vac. Sci. Technol. B* **23**, 772 (2005).

¹⁰H. J. Jeong, S. C. Lim, K. S. Kim, and Y. H. Lee, *Carbon* **42**, 3003 (2004).

¹¹W. A. de Heer, J. M. Bonard, K. Fauth, A. Châtelain, L. Forró, and D. Ugarte, *Adv. Mater. (Weinheim, Ger.)* **9**, 87 (1997), and references cited therein.

¹²H. Schmid and H. W. Fink, *Appl. Phys. Lett.* **70**, 2679 (1997).

¹³Y. Saito, K. Hamaguchi, T. Nishino, K. Hata, K. Tohji, A. Kasuya, and Y. Nishina, *Jpn. J. Appl. Phys., Part 2* **36**, L1340 (1997).

¹⁴Q. H. Wang, T. D. Corrigan, J. Y. Dai, R. P. H. Chang, and A. R. Krauss, *Appl. Phys. Lett.* **70**, 3308 (1997).

¹⁵N. I. Sinitsyn, Y. V. Gulyaev, G. V. Torgashov, L. A. Chernozatonskii, Z. Y. Kosakovskaya, Y. F. Zakharchenko, N. A. Kiselev, A. L. Musatov, A. I. Zhanov, S. T. Mevlyut, and O. E. Glukhova, *Appl. Surf. Sci.* **111**, 145 (1997).

¹⁶J. M. Bonard, F. Maier, T. Stöckli, A. Châtelain, W. A. de Heer, J. P. Salvetat, and L. Forró, *Ultramicroscopy* **73**, 7 (1998).

¹⁷Q. Chen and L. Dai, *J. Nanosci. Nanotechnol.* **1**, 43 (2001).

¹⁸X. B. Wang, Y. Q. Liu, P. A. Hu, G. Yu, K. Xia, and D. B. Zhu, *Adv. Mater. (Weinheim, Ger.)* **14**, 1557 (2002).

¹⁹A. Cao, R. Baskaran, M. J. Frederick, K. Turner, P. M. Ajayan, and G. Ramanath, *Adv. Mater. (Weinheim, Ger.)* **15**, 1105 (2003).

²⁰S. Huang and A. W. H. Mau, *Appl. Phys. Lett.* **82**, 796 (2003).

²¹Y. Yang, S. Huang, H. He, A. W. H. Mau, and L. Dai, *J. Am. Chem. Soc.* **121**, 10832 (1999).

²²Z. J. Zhang, B. Q. Wei, G. Ramanath, and P. M. Ajayan, *Appl. Phys. Lett.* **77**, 3764 (2000).

²³Y. Xia and G. M. Whitesides, *Angew. Chem.* **110**, 568 (1999).

²⁴S. Huang, A. W. H. Mau, T. W. Turney, P. A. White, and L. Dai, *J. Phys. Chem. B* **104**, 2193 (2000).

²⁵S. Huang, L. Dai, and A. W. H. Mau, *J. Phys. Chem.* **103**, 4223 (1999).

²⁶J. Yang, L. Dai, and R. A. Vaia, *J. Phys. Chem. B* **107**, 12387 (2003).

²⁷S. Huang, A. W. H. Mau, T. W. Turney, P. A. White, and L. Dai, *J. Phys. Chem. B* **104**, 2193 (2000).

²⁸L. Dai, P. He, and S. Li, *Nanotechnology* **14**, 1081 (2003).

²⁹A. Patil, L. Li, L. Dai, M. Casavant, and K. Strong, *J. Soc. Inf. Disp.* **13/9**, 709 (2005).

³⁰Q. Chen, L. Dai, M. Gao, S. Huang, and A. W. H. Mau, *J. Phys. Chem. B* **105**, 618 (2001).